Shell Models with Enhanced Kinematics for Finite Elements in Sheet Metal Forming Simulations

Tobias Willmann[1], Manfred Bischoff[1]

[1]Institute for Structural Mechanics
University of Stuttgart
Pfaffenwaldring 7, 70550 Stuttgart, Germany
{willmann;bischoff}@ibb.uni-stuttgart.de

1 Abstract

Beyond the shell model of Reissner and Mindlin, which is available in LS-DYNA® for example in shell ELFORM=2/16, there have been many developments in the field of 3d-shell models in recent years [1]. 3d-shell models can be beneficial in sheet metal forming simulations because they allow for three-dimensional stress states. 3d-shell elements are available in LS-DYNA®, e.g. ELFORM=25. In the doctoral dissertation of Fleischer[2] it has been found that under certain conditions this element formulation suffers from an artificial stiffening effect. Although this finding dates back to 2009, this phenomenon has remained unexplained so far. In this contribution, the authors explain the reason for this stiffening effect and show a possibility to remove it. Moreover, an outlook on the development of higher order shell models for sheet metal forming simulation is given.

2 Introduction

To predict the result of sheet metal forming processes precisely using finite element simulations, a detailed description of both the material and the structure is necessary. In sheet metal forming simulations, the structure is usually modeled using shell elements. This paper briefly explains some of the most commonly used shell models and relates them to shell elements available in LS-DYNA®. In the further course, we carry out a benchmark study to show that state of the art shell elements reach their limit of predictive capability in certain sheet metal forming applications. Finally, we present two shell element formulations and compare them to existing formulations available in LS-DYNA®.

3 Shell Model Overview

3.1 State of the Art Shell Models

Many of the widely used shell finite elements base on the assumptions of Reissner and Mindlin. They state, amongst others, that straight cross-sectional fibres remain straight and transverse normal stresses are negligible. Moreover, there is no explicit kinematic description of the thickness change of the shell during deformation. For many applications, these assumptions are reasonable. However, in critical sheet metal forming situations where local effects occur, as for example extreme thinning or bending over small radii, these assumptions are not valid anymore and therefore the elements reach their limit of applicability. The model of Reissner and Mindlin is present in LS-DYNA® for example in shell ELFORM=2 or ELFORM=16.

3.2 3d-shell Models

Compared to the Reissner-Mindlin shell model, 3d-shell models include thickness change and transverse normal stresses. Examples for elements based on 3d-shell models are director based 6- and 7-parameter shells or solid shell elements based on 8-node bricks [1]. Due to their enhanced kinematics, 3d-shell models offer a greater modeling flexibility, but they still impose constraints. One of these constraints is that the distribution of transverse normal stresses in thickness direction is limited and can be at most linear. Another important constraint is that straight cross sections remain straight as they also do in the model of Reissner and Mindlin. A relevant difference compared to the Reissner-Mindlin model is that 3d-shell models are able to represent a fully 3d-stress state and therefore need appropriate material laws. Examples for shell elements based on 3d-shell-models in LS-DYNA® are shell ELFORM=25 and ELFORM=26.

© 2019 Copyright by DYNAmore GmbH

3.3 Higher Order Shell Models

Compared to the shell models explained before, higher order models allow for a deformable cross section and a higher order stress distribution in thickness direction. Seen from a theoretical point of view, the deformation of the cross section and the stress distribution in thickness direction can be modeled by any desired linear combination of polynomials. However, adding additional deformation modes adds additional degrees of freedom to the element formulation and increases computational costs. Depending on the desired field of application, different choices for the enhancement of the deformation can be reasonable.

Figure 1 motivates the development of higher order shell elements for sheet metal forming simulations. The image on the left side sketches a simplified deep drawing situation. The sheet (green) is drawn out of the rigid tools (grey). The sheet is modeled with an elastic-plastic material law and friction between sheet and tools is considered. A fine solid mesh resolves effects in thickness direction. The image in the middle shows the normal stress in horizontal direction in the sheet as a fringe plot. The diagram on the right side of Figure 1 shows the stress in horizontal direction at the position of the dashed line plotted against the sheet thickness. The shape of this stress distribution is similar to a parabola. Neither state of the art shell models nor 3d-shell models are able to represent such as stress state correctly. Both models assume this stress component to be constant over the thickness in this load case. To model such effects, higher order shell models are necessary, which include the respective deformation modes in their kinematic assumptions. Besides this enhancement in modeling friction-dominated situations as shown here, higher order shell models can also be beneficial for bending dominated situations.

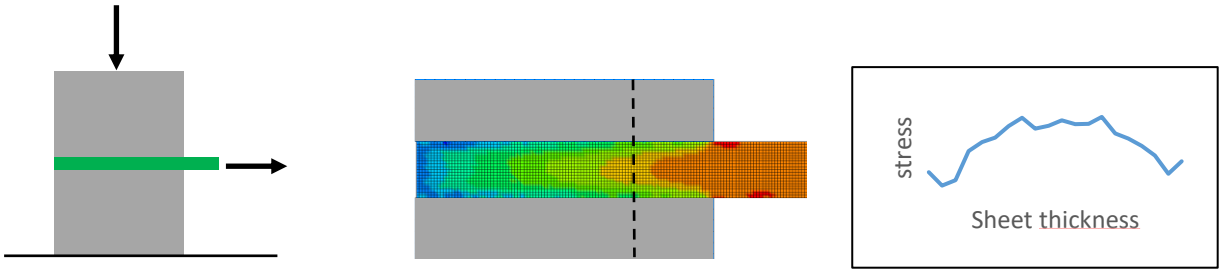

Fig.1: Sketch of a sheet being drawn out of forming tools (left). Stress distribution in the sheet as a fringe plot (middle) and plotted as a curve over the sheet thickness (right).

4 A Benchmark for Shell Elements in Sheet Metal Forming Simulations

4.1 Test setup

Figure 2 shows a virtual ring test performed by [2]. The ring is fixed at point A and virtually sliced into two parts at point B. Displacement boundary conditions *u(t)* are applied as shown in Figure 2. These boundary conditions cause a continuous decrease of the ring's radius and thus bending with increasing curvature occurs. The situation at point A is comparable to the load that occurs in a sheet that is bent over a small radius compared to its thickness. Such situations occur in many practically relevant sheet metal forming operations. Figure 3 shows a 3d-view of the virtual ring test to clarify the test geometry.

This test is a benchmark for element behavior in case of bending over small radii as it appears in sheet metal forming simulations. The advantages of this test compared to simulation of real forming operations is that no additional tools need to be modeled and no contact algorithm is necessary. This facilitates an isolated evaluation of the elements' performance.

To emphasize that the error in the simulation of this test with shell elements only emanates from the element formulation and does not emanate from other factors such as complicated material laws, a simple elastic material law (MAT_001) is used in this test. Poisson's ratio is close to 0.5 and plane strain conditions are applied to model almost incompressible behavior as it also appears in plastic deformation.

© 2019 Copyright by DYNAmore GmbH

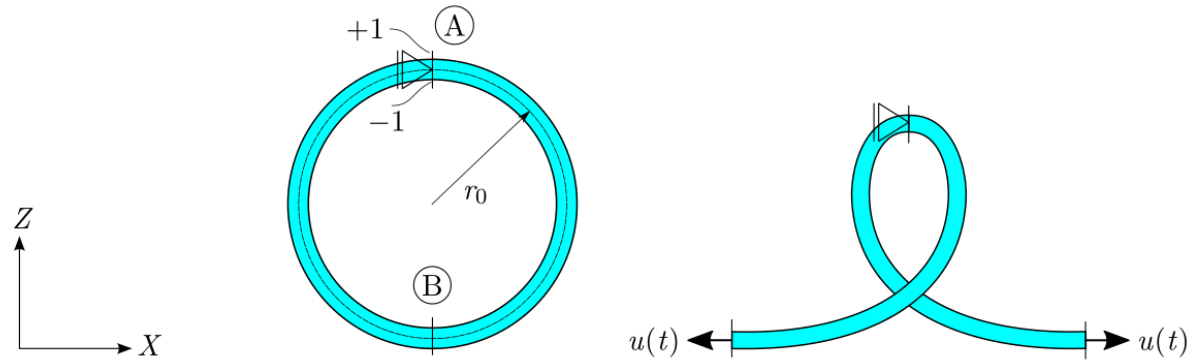

Fig.2: Virtual ring test: Undeformed configuration (left) and deformation after application of boundary conditions (right).

Fig.3: 3-d view of the virtual ring test.

Before discussing the results for shell elements, we present the reference solution. The numerical reference solution for this test is a fine-meshed simulation using solid elements. Figure 4 shows the deformation of the ring at the end of the simulation in the area around point A. This deformation is obtained from the reference solution. “-1” and “+1” indicate the lower and upper face of the sheet, respectively (cf. Figure 2). For comparison, there are straight red dashed lines drawn into the figure. The cross section in case of large bending deformations does not remain straight in this test.

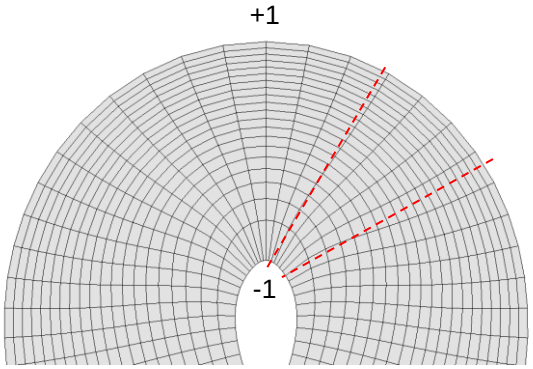

Fig.4: Cross sections close to A do not remain straight in the virtual ring test (deformed cross sections are shown in black, red dashed lines are straight lines).

© 2019 Copyright by DYNAmore GmbH

Figure 5 shows a cut through a metal sheet being drawn over a drawbead from left to right. In this case, the sheet is simulated using five solid elements in thickness direction. Before the sheet has passed the drawbead, the cross sections are straight (left side). After being drawn over the drawbead, the sheet shows an S-shaped deformation of the cross section. This illustrates that the deformation of the cross sections occurring in the virtual ring test is not artificial but also appears in practical forming examples.

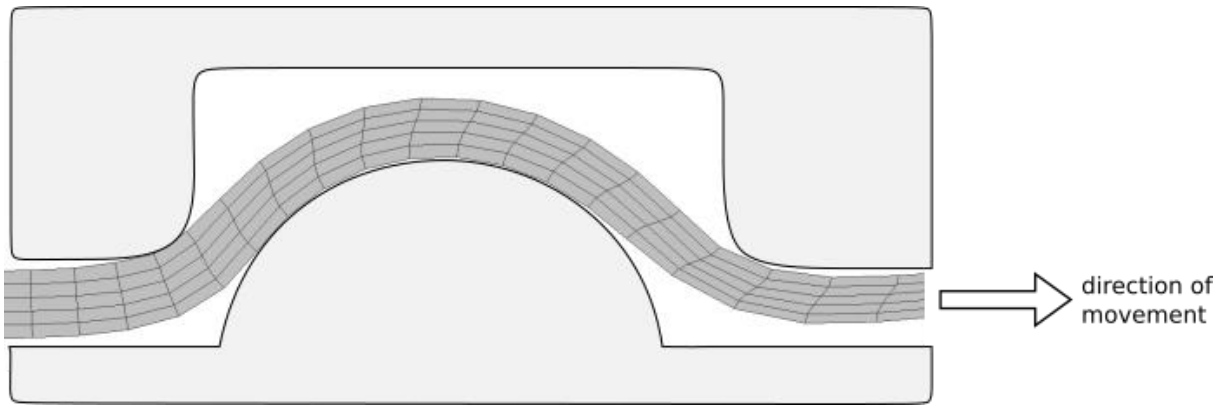

Fig.5: Cut through a metal sheet drawn over a drawbead.

4.2 Test results for shell elements

Figures 6 to 8 show, besides the reference solution, simulation results of four different shell element formulations. We discuss in particular S2 and S25 in this chapter. The other two formulations, S25+ and 3DBM_7, are discussed in the following chapter. S2 refers to shell ELFORM=2 in LS-DYNA® and S25 refers to shell ELFORM=25.

Figure 6 shows the force that is necessary to apply the deformation *u(t)*. The Figure shows that at the beginning, i.e. in case of small deformations, all element formulations yield the same result. At some point, S25 starts to behave far too stiff. This is due to a stiffening effect, which only has an impact in case of large strains.

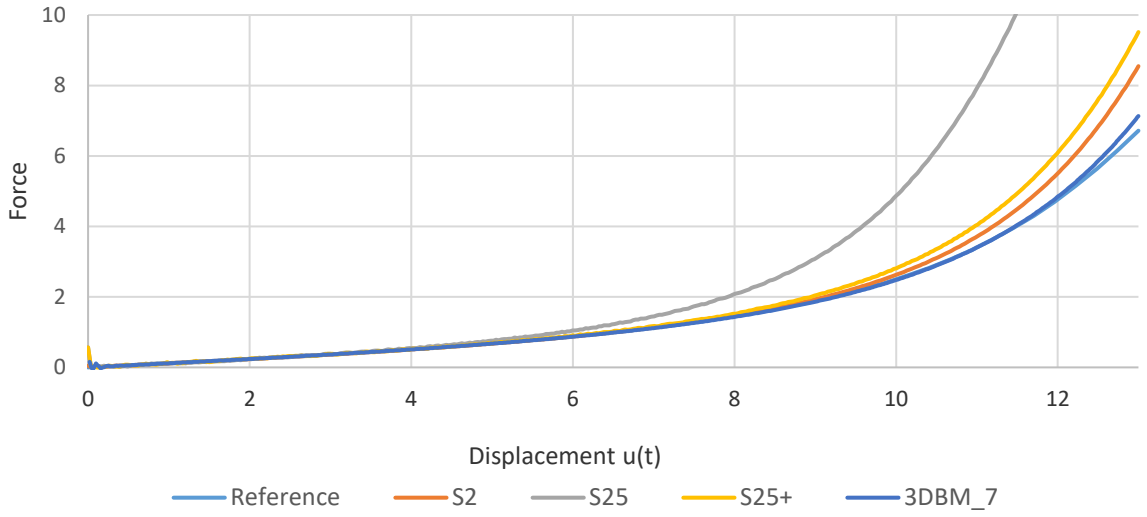

Fig.6: Force displacement diagram for the virtual ring test.

© 2019 Copyright by DYNAmore GmbH

Shell element S2, which is representing the standard shell models in this test, performs better, but as soon as the deformation becomes very large, there is a notable difference between the solution of S2 and the reference solution. There are several reasons for this difference. As shown before, the cross section does not remain straight in the reference solution of this test. As S2 is based on the assumptions of Reissner and Mindlin, its cross section remains straight. Furthermore, bending is modeled only linearly in this element. This assumption is valid in case of small bending deformations but it is not valid in case of large bending deformations. Finally, transverse normal stresses are assumed to be zero in state of the art shell models. This is also not true for large bending deformations.

5 Current research in Shell Element Development

5.1 Improved Shell ELFORM=25 without Stiffening Effect

Fleischer [2] originally observed the stiffening effect shown in Figure 6. An explanation for this stiffening effect as well as a method how to solve it remained unavailable until recently. Due to a defect in the kinematical assumption of the underlying shell model, ELFORM=25 is unable to represent bending correctly in case of an almost incompressible material law. It is possible to interpret the stiffening effect as higher order Poisson thickness locking.

The authors developed a slightly modified version of ELFORM=25. In all figures shown in this paper, we denote this improved element as S25+. Figure 6 shows that the stiffening effect was successfully eliminated, as the force level is comparable to state of the art shell elements.

Figure 7 shows the distribution in thickness direction of the in-plane normal stress, i.e. the stress in x-direction in the coordinate system in Figure 1. The stress is evaluated at point A at the end of the simulation. The left part of the figure includes the curve representing S25. It is clearly visible that the stiffening effect dominates the stress distribution and yields unphysically high stresses. To be able to compare the remaining curves to each other, the diagram on the right side of Figure 7 shows the remaining curves without the curve representing S25.

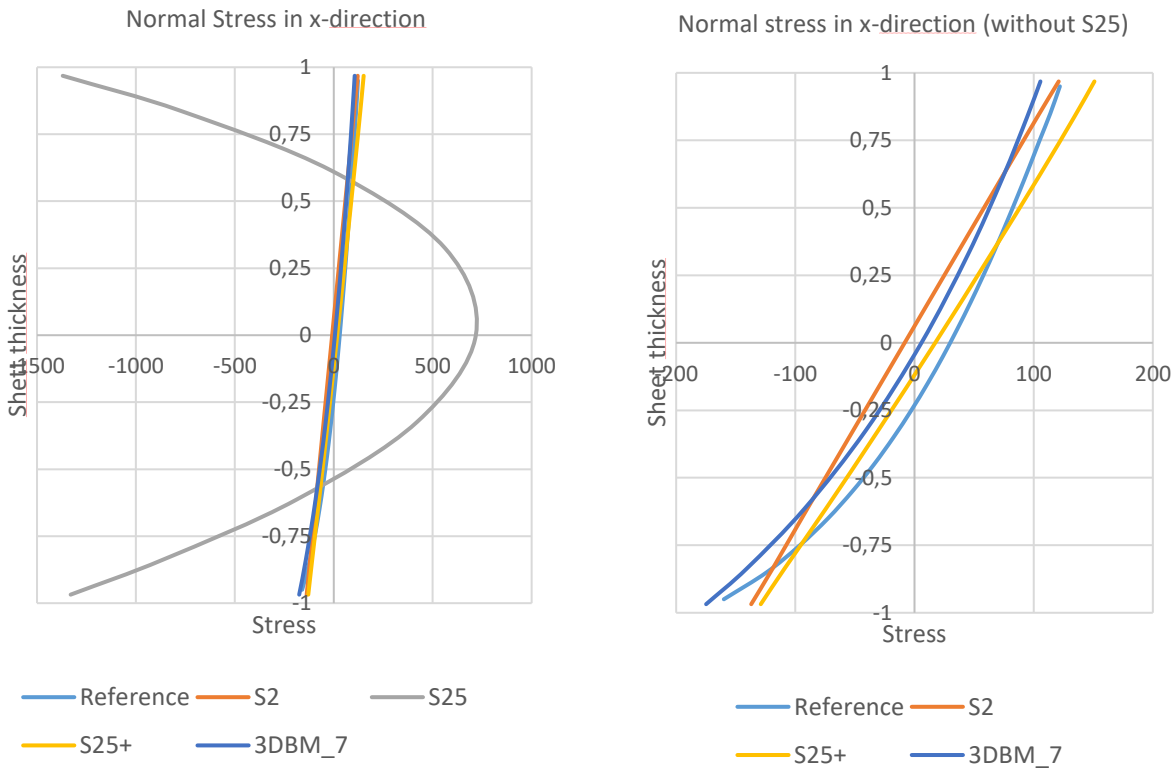

Fig.7: Distribution over the thickness of normal stresses in x-direction with and without S25.

© 2019 Copyright by DYNAmore GmbH

Both the force displacement curve and the stress plot indicate that S25+ performs much better than S25 in case of large bending deformations with almost incompressible material. This improvement is already available in an LS-DYNA® developer version. To use it, one has to choose ELFORM=25 in *SECTION_SHELL and set the value of IDOF to 11 (continuous thickness field) or 12 (discontinuous thickness field). Regarding computational costs, there is no significant difference between S25 and S25+. Furthermore, pre- and post-processing in S25+ is identical to S25 so that it does not require any changes in existing workflows.

5.2 Improved 3d-Shell Elements

The authors developed another shell element, which we refer to as 3DBM_7 in this paper. The underlying shell model is a 3d-shell model. The main difference of 3DBM_7 compared to S25 and 25+, which also implement a 3d-shell model, is that 3DBM_7 models bending nonlinearly. This is an important improvement, especially in case of large bending deformations. 3DBM_7 is a fully integrated shell element, which uses the ANS-method [3] to avoid transverse shear locking. Furthermore, an incompatible quadratic displacement field avoids Poisson thickness locking.

The simulation results of 3DBM_7 are included in Figures 6, 7 and 8. 3DBM_7 can reproduce the force displacement curve of the reference solution almost exactly, even in case of large bending deformation. The in-plane normal stress in x-direction in Figure 7 approximates the reference solution well. Among the element formulations discussed in this paper, 3DBM_7 is the only one that is able to reproduce the nonlinear shape of the reference stress distribution.

Figure 8 shows the transverse normal stresses evaluated at point A at the end of the simulation. As stated by the Reissner-Mindlin assumptions, the transverse normal stress distribution in shell element S2 is exactly zero. The stress distribution of S25+ looks somehow artificial and does not approximate the reference solution well. This is an indication that these stresses are a result of some numerical artifact. The approximation of the transverse normal stresses by 3DBM_7 is better. As expected, the transverse normal stress is constant in thickness direction for element formulation 3DBM_7.

It is worth noting that the complexity of the material law influences the quality of the stress representation. 3DBM_7 might not reproduce the reference solution for more complex material laws as good as it does for an elastic material law. Nevertheless, we expect that 3DBM_7 outperforms the other formulations also in simulations using more complex material laws.

The only available implementation of 3DBM_7 is in the authors' own finite element code. Therefore, it is not possible to provide a realistic comparison of computational costs between 3DBM_7 and the elements implemented in LS-DYNA®.

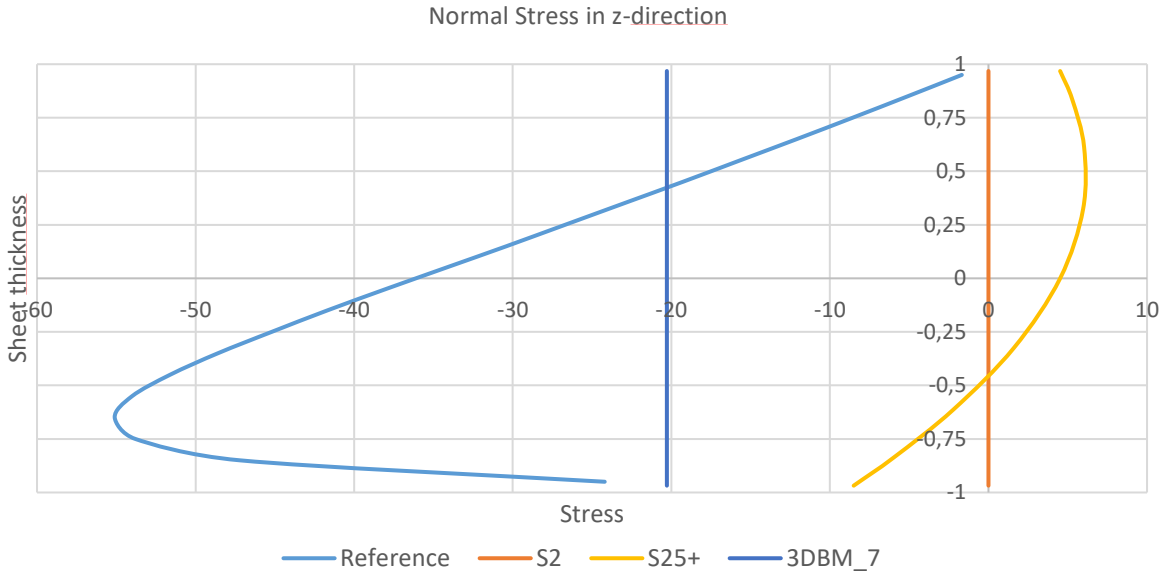

Fig.8: Normal stress in z-direction at point A of the virtual ring test at the end of the simulation.

© 2019 Copyright by DYNAmore GmbH

6 Conclusion

In this paper, a benchmark test was carried out to analyze the performance of shell ELFORM=2 and ELFORM=25 in LS-DYNA®. Furthermore, we presented two new element formulations. S25+ is an improved variant of shell ELFORM=25 that does not suffer any more from the stiffening effect observed in [2]. Element formulation 3DBM_7 performs very well in case of large bending deformation and provides improved through-the-thickness stress predictions.

7 Acknowledgements

The present study was supported within project No. 09/117 of the European Research Association for Sheet Metal Processing e.V. and as project No. 19797N within the framework of the AiF (Program for the Promotion of Industrial Community Research of the Federal Ministry for Economic Affairs and Energy) of Germany. This support is gratefully acknowledged.

The authors would like to thank Bastian Oesterle and Anton Tkachuk, supported by DFG Research Grant TK 63/1-1, for the fruitful discussions within the emergence of this work.

8 Literature

[1] Bischoff, M., Irslinger, J. Ramm, E.: “Models and Finite Elements for Thin-Walled Structures“, Encyclopedia of Computational Mechanics. Second Edition, E. Stein, R. de Borst, T.J.R. Hughes (eds.), 2018

[2] Fleischer, M.: “Absicherung der virtuellen Prozesskette für Folgeoperationen in der Umformtechnik“, Dissertation, Technische Universität München, 2009

[3] Bathe, K.J., Dvorkin, E.N.: „A formulation of general shell elements – The use of mixed interpolation of tensorial components“, International Journal for Numerical Methods in Engineering 22, 1986

© 2019 Copyright by DYNAmore GmbH